Supporting Information

The atomic pair distribution function (PDF) is a total scattering technique that provides the probability of finding pairs of atoms at specific distances(Egami & Billinge, 2003). The experimental PDF function $G_{exp}(r)$ is obtained from the Fourier transform of the normalized and corrected scattering intensity $S(Q)$ obtained up to a high scattering vector Q ($Q = \frac{4\pi\sin(\theta)}{\lambda}$).

$$Gexp(r) = \frac{2}{\Pi} \int_{Qmin}^{Qmax} Q[S(Q) - 1]\, sin(Qr)\, dQ \qquad (1)$$

The PDF can be also calculated using:

$$Gcalc(r) = \frac{1}{rN} \sum_{i,j \neq i} \frac{fifj}{\langle f \rangle^2} \delta(r - rij) - 4\pi r \rho_0 \qquad (2)$$

Where f_i and f_j is the atomic scattering factor for atoms i and j respectively, and ρ_0 is the average atom-pair density. This technique allows the refinement of structural models through programs such as PDFfit2 and its user interface PDFgui (Farrow *et al.*, 2007). One of the improvements of these programs is the ability to refine the average nanoparticle sizes by attenuating the bulk calculated PDF by a function simulating a monodisperse spherical form factor. (Farrow *et al.*, 2014; Shi *et al.*, 2013) using:

$$G(r)_{nanoparticle} = G(r)_{Bulk} \gamma_0(r) \qquad (3)$$

Where $\gamma_0(r)$ is expressed as:

$$\gamma_0(r) = \left[1 - \frac{3r}{2D} + \frac{1}{2}\left(\frac{r}{D}\right)^3\right] H(D - r) \qquad (4)$$

and H is a Heaviside step function which ensures that the signal is zero at distances larger than the particle diameter.

The related differential pair distribution function (d-PDF) technique allows the isolation of the contribution of a particular component of a sample. This is done in supported materials by subtracting directly the PDF of the support. Recent studies using PDF analysis have shown that it is a feasible technique to obtain the structural information of supported metal catalysts (Chupas *et al.*, 2007; Chupas *et al.*, 2009; Zhao *et al.*, 2011; Newton *et al.*, 2012; Farrow *et al.*, 2014; Shi *et al.*, 2013) Below we describe the Pt d-PDF results of two Pt/NaX samples reduced at 350°C in a quartz furnace tube and in a Kapton®-HN type polyimide capillary.

S1. Methodology

S1.1. Synchrotron Data Collection

The X-ray scattering experiments were carried out at the 11-ID-B beamline of the Advanced Photon source at Argonne National Laboratory. Diffraction data were collected using an area two dimensional amorphous silicon based flat panel detector from Perkin-Elmer. A sample to detector distance of 20 cm and a maximum 2-theta scan angle of 50° were used. The powder samples were analyzed in transmission geometry, with an X-ray wavelength of λ=0.2128 Å. The two-dimensional data were integrated and converted to one-dimensional intensity versus 2-theta using the FIT2D program (Hammersley *et al.*, 1996). The PDFgetX3 program (Juhás *et al.*, 2013) was used to obtain the experimental *G(r)* of NaX and the reduced Pt/NaX, subtracting only the corresponding capillary as background. To obtain the differential PDFs (d-PDFs), the *G(r)* of the NaX was substracted from the *G(r)* of the reduced Pt/NaX. The data were truncated at finite minimum and maximum values of the momentum transfer, of Qmax = 13.3 $Å^{-1}$ and Qmin=2.4 $Å^{-1}$

S1.2. Refinements of the differential Pt PDFs

A value for the PDF refinement variables Qdamp and Qbroad were obtained by refining a CeO2 standard. The value of the Qbroad was fixed, but Qdamp was allowed to refine further.

The d-PDFs were used to refine the structure of the Pt nanoparticles assuming an fcc symmetry using the program PDFgui, (Farrow *et al.*, 2007). The scale and Qdamp were refined first. The structural parameters refined were: peak sharpening (delta 2), lattice parameters, isotropic thermal factors and average particle diameters. The refinements were done up to an interatomic distance of 40 Å.

S1.3. Refinement of multiple phases

The multiphase refinement was carried out by first refining the support structure (NaX) using the support PDF. Global and phase scales, Qdamp and structural parameters (delta 1, lattice parameters, isotropic thermal factors, extra-framework positions, framework positions and extra-framework occupancies) were refined. The resulting support structure was then used as a starting point for the refinement of the Pt/NaX PDF. The global scale and phase scales were refined first to estimate the phase concentrations. The refinement continued with Qdamp and refinement of the Pt phase structural parameters: delta 2, lattice parameters, isotropic thermal factors and Pt particle diameter.Then the NaX phase structural parameters were refined: delta 1, lattice parameters, isotropic thermal factors, extra-framework positions, framework positions and extra-framework occupancies. The multiphase refinement was done up to an interatomic distance of 40 Å.

Figure S1 PDF of the zeolite support NaX (solid line), the Pt/NaX catalyst (dashed line) and the difference (offset below) of the sample reduced in a quartz reactor.

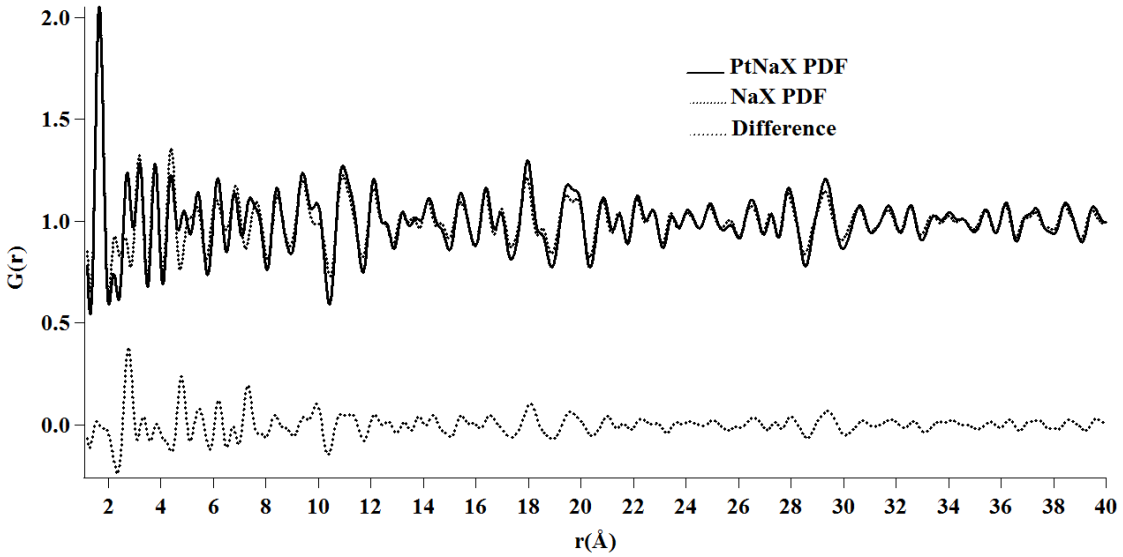

Figure S2 PDF of the zeolite support NaX (solid line), the Pt/NaX catalyst (dashed line) and the difference (offset below) of the sample reduced in a Kapton®-HN type capillary

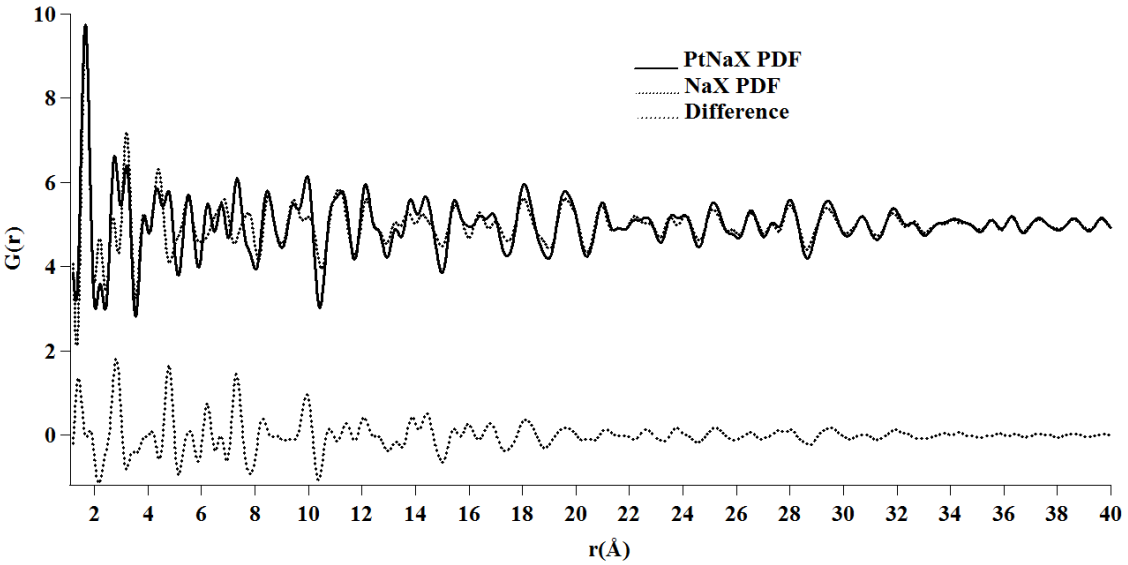

S2. Results

Figure S3 shows that the d-PDFs for the samples reduced in a quartz furnace tube and a Kapton®-HN type polyimide capillary follow similar trends but the peaks of the sample reduced in the polyimide are, in general, more intense. This tendency in this technique is representative of larger Pt nanoparticles. The diameter of the crystalline nanoparticle as obtained by refining these Pt d-PDF were 24.4 Å (PDFgui residual Rwp=35.4%) and 37.6 Å (Rwp= 28.3%) for the sample reduced in a quartz furnace tube and in a Kapton®-HN type capillary, respectively (Figures S4 and S5).

The refinement of the Pt nanoparticles grown in the quartz tube yields a worse agreement because there is more noise at high-r. This is probably because in this sample a larger fraction of the nanoparticles are located within the pores of the support distorting its local structure. To overcome this problem a multiphase PDF refinement was carried out to 40 Å (Figure S6). The refined diameter of the crystalline nanoparticles was 23.1 Å (Rwp=31.8%) which is similar to the value obtained by d-PDF but with a better agreement.

The difference in the average sizes between the two samples is consistent with the differences found with STEM. The values cannot be compared directly with the average sizes obtained by HAADF-STEM (16(6) Å for the quartz tube and 36(47) Å for the Kapton capillary) because of the inherent differences in the techniques. As an imaging technique HAADF-STEM results are affected by the sampling and separation of the nanoparticles and, as a scattering technique, PDF results are more affected by the presence of large ordered nanoparticles. New algorithms are being developed to obtain more realistic structural models and particle size distributions through refinement of the PDF. (Farrow *et al.*, 2014)

Figure S3 Pt Differential PDFs of samples reduced in the Kapton®-HN type capillary (solid line) and in a quartz reactor (dashed line).

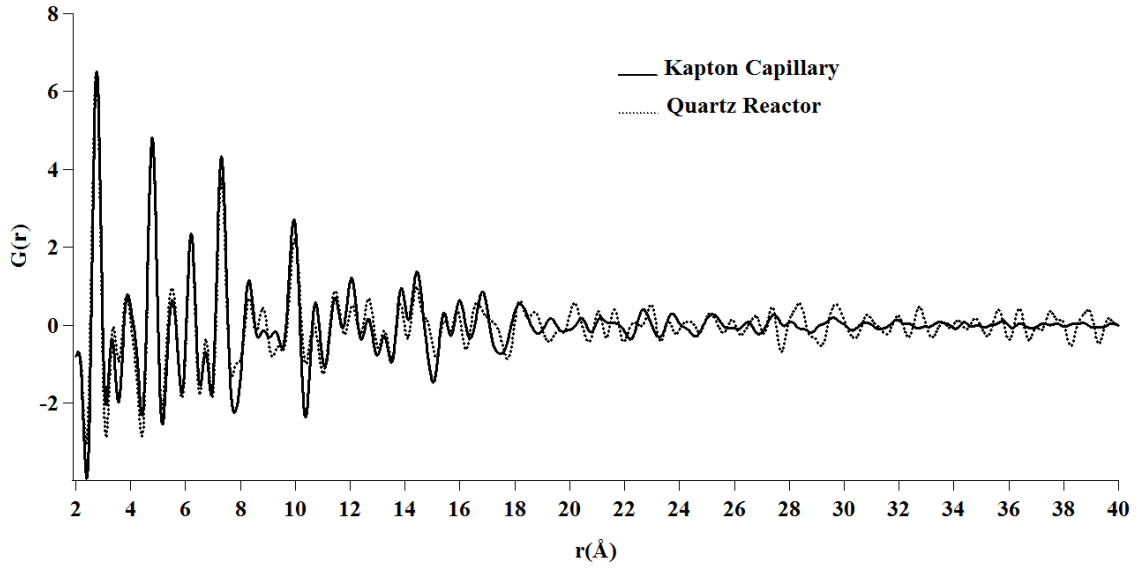

Figure S4 Fit of the Pt d-PDF of the sample reduced in the quartz reactor. Experiment (solid line),calculated (dashed line) and difference (offset below)

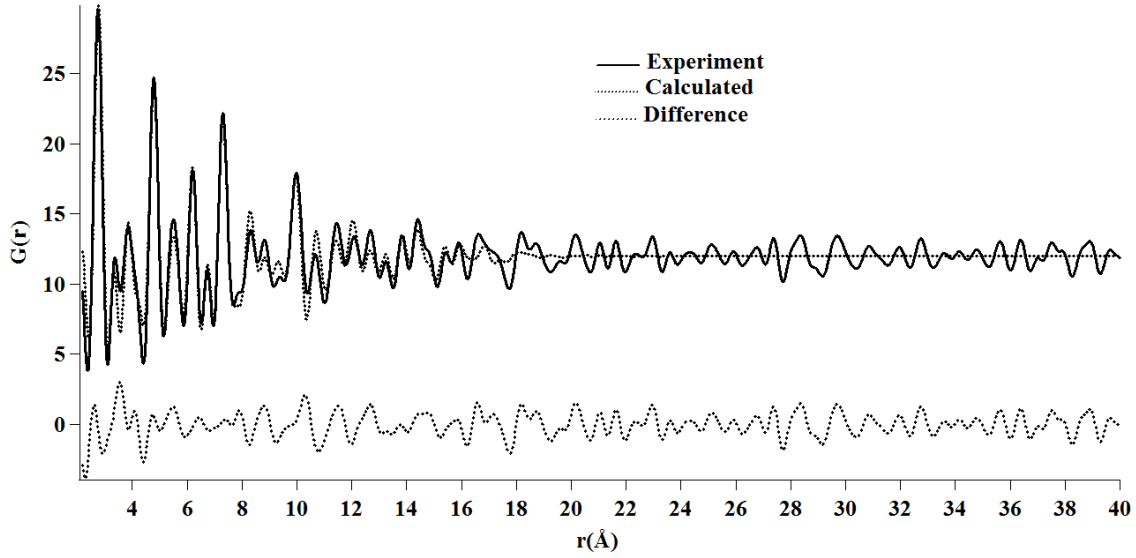

Figure S5 Fit of the Pt d-PDF of the sample reduced in a Kapton®-HN type capillary. Experiment (solid line),calculated (dashed line) and difference (offset below)

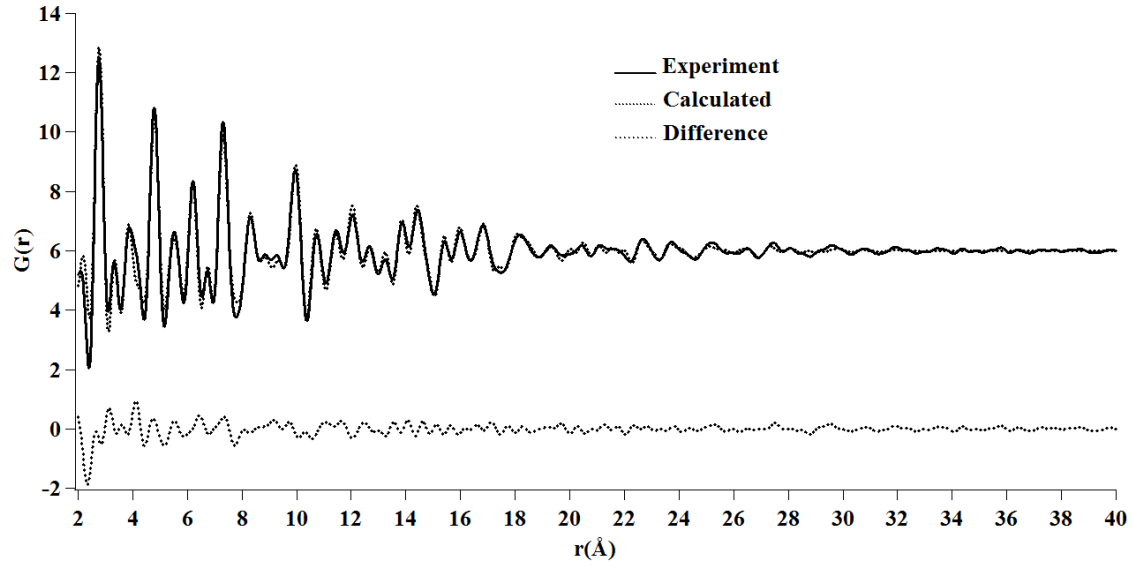

Figure S6 Fit of the multiphase PDF of the sample reduced in the quartz reactor. Experiment (solid line),calculated (dashed line) and difference (offset below)

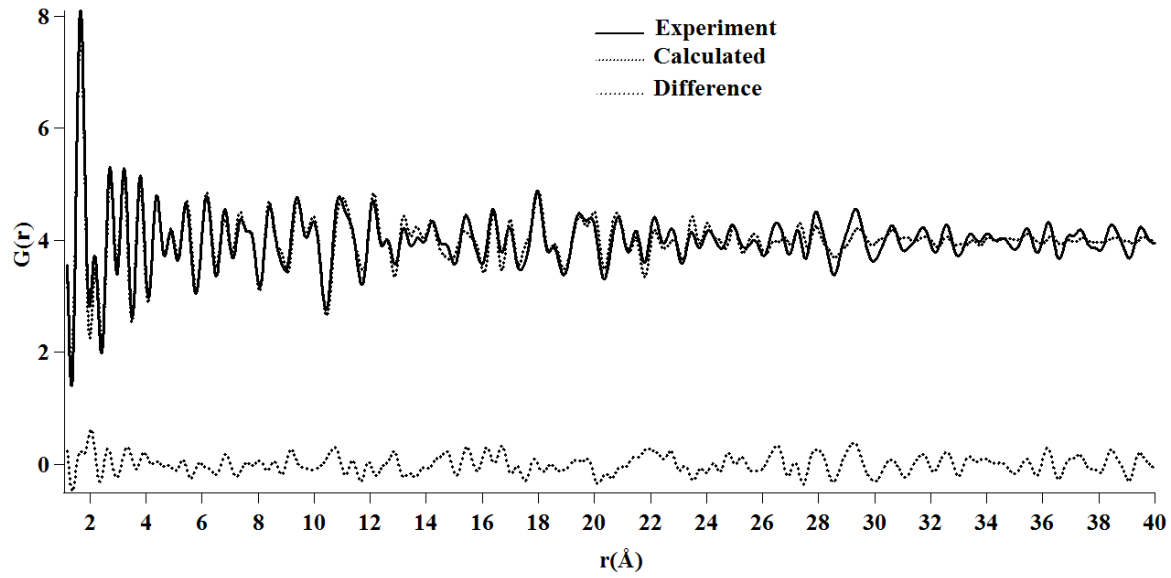

S3. References

Chupas, P. J., Chapman, K. W., Chen, H. & Grey, C. P. (2009). *Catalysis Today* **145**, 213-219.

Chupas, P. J., Chapman, K. W., Jennings, G., Lee, P. L. & Grey, C. P. (2007). *Journal of the American Chemical Society* **129**, 13822-13824.

Egami, T. & Billinge, S. J. L. (2003). *Underneath the Bragg Peaks:Structural Analysis of Complex Materials*, 1st ed. Amsterdam: Elsevier.

Farrow, C. L., Juhas, P., Liu, J. W., Bryndin, D., Božin, E. S., Bloch, J., Th, P. & Billinge, S. J. L. (2007). *Journal of Physics: Condensed Matter* **19**, 335219.

Farrow, C. L., Shi, C., Juhás, P., Peng, X. & Billinge, S. J. L. (2014). *Journal of Applied Crystallography* **47**, 561-565.

Hammersley, A. P., Svensson, S. O., Hanfland, M. & Hauserman, D. (1996). *High Pressure Research* **14**, 235-248.

Juhás, P., Davis, T., Farrow, C. L. & Billinge, S. J. L. (2013). *Journal of Applied Crystallography* **46**, 560-566.

Newton, M. A., Chapman, K. W., Thompsett, D. & Chupas, P. J. (2012). *Journal of the American Chemical Society* **134**, 5036-5039.

Shi, C., Redmond, E. L., Mazaheripour, A., Juhas, P., Fuller, T. F. & Billinge, S. J. L. (2013). *The Journal of Physical Chemistry C* **117**, 7226-7230.

Zhao, H., Nenoff, T. M., Jennings, G., Chupas, P. J. & Chapman, K. W. (2011). *The Journal of Physical Chemistry Letters* **2**, 2742-2746.